Progress In Electromagnetics Research C, Vol. 81, 191–197, 2018

Scalable Preparation of Broadband Ultrablack Graphite Nanoneedle Surfaces through Self-Masked Etching

Tingbiao Guo[1], Yaoran Sun[1], Sailing He[1, 2], Jiang Yang[1], Mengzhu Hu[1], Wen Mu[3], and Julian Evans[1, *]

Abstract—Ultrablack materials play an essential role in astronomical observation and many thermal applications. Many material systems such as vertically aligned carbon nanotubes have produced extraordinarily high absorption, but require complicated fabrication. Here we report a single step self-masked etching process performed on compressed-coal graphite plates on a silicon substrate, which produces an ultrablack material with 0.7% hemispherical reflectance in the visible region and specular reflectance below 0.7% between 850 nm and 10 µm. Nanoscopic pieces of silicon are ripped off the substrate and deposit on the graphite resulting in carbon nanoneedle structures, which grow linearly with etching time reaching a height of 5.7 µm after 60 minutes.

1. INTRODUCTION

An ideal black body, which absorbs all electromagnetic waves at all wavelengths, plays an essential role in the development of modern physics and has numerous technological applications [1–3]. While an ideal black body is not achievable, a variety of material platforms have enabled ultrablack materials that have nearly zero reflection and emit radiation in accordance with the black body spectrum. Ni-P [4, 5], vertically aligned carbon nanotubes [6, 7], and noble metals [8] are the most prominent established methods for the production of ultrablack materials. These ultrablack materials have many exciting applications in thermophotovoltaics [9], thermal detectors [10], infrared imaging [11, 12] and thermal management [13]. Since room temperature black-body's radiation has a peak around a wavelength of 10-µm, broadband ultrablack material (from VIS to mid-IR) is a good system for radiative heat transfer especially in the outer space where radiative transfer is the only way to dissipate heat.

Absorbers based directly on silicon are an attractive idea, since silicon is the most widely-used material in the semiconductor and solar industries. Many methods, such as femtosecond-laser pluses [14], wet-chemical etching [15], dry-etching [16], have been applied to fabricate silicon-based absorbers. However, all these methods are limited to a relatively narrow band by the material properties of silicon. The typical absorption band for silicon-based absorbers is from 350 nm to 2000 nm.

Carbon is an ideal material for absorption since the π-band's transitions are active at any wavelength longer than the hard UV region. Vertically aligned carbon nanotube arrays (VANTA) are the best known material for approaching perfect absorption. They have been used to get an ultra-black absorber across a wide spectral range from UV (200 nm) to far infrared (200 µm) with the reflectance well below 1% [6]. However, their production requires elevated temperatures and complicated techniques and the final product is somewhat fragile. We have previously reported a flexible ultra-black absorber

Received 30 November 2017, Accepted 14 February 2018, Scheduled 21 February 2018

* Corresponding author: Julian Evans (julian@coer-zju.org).

[1] Centre for Optical and Electromagnetic Research, Zhejiang Provincial Key Laboratory for Sensing Technologies, Zhejiang University, Hangzhou 310058, People's Republic of China. [2] Department of Electromagnetic Engineering, Royal Institute of Technology, Stockholm S-100 44, Sweden. [3] College of Optical Science and Engineering, Zhejiang University, Hangzhou 310027, People's Republic of China.

consisting of smooth [17] or hairy [18] nanocones produced through nanoparticle and photoresist masked etching of highly ordered pyrolytic graphite (HOPG) respectively. The hairy nanocone material is of comparable quality to VANTA materials of a similar thickness, but is limited by the requirement of a high quality initial carbon material. Other allotropes of carbon such as vitreous carbon foam, graphene and pyrolytic carbon have been reported as strong absorbers in many wavelength ranges. Vitreous carbon foams have shown reflectance below 1% in the THz range [19]. Graphene sandwich structures show a reflectance around 1% and absorbance around 85% in GHz range [20]. Amorphous pyrolytic carbon coated ultrablack silicon material has reflectance as low as 0.5% in the visible range [21].

Here we report an ultrablack absorber made from a compressed-coal graphite plate by self-masked [22] dry-etching technique where nanoscopic silicon is sputtered onto the graphite surface from the substrate resulting in the growth of high-quality vertical carbon nanoneedles. This method uses a low-cost graphite plate and the process is very simple and scalable. The absorber shows a broadband absorption from the visible (450 nm) to the mid-infrared (10 μm) range with a reflectance below 1%. The formation and composition of the nanoneedle structures on the surface are explored by using XPS elemental analysis, which confirms that the nanoneedles emerge from the self-mask effect during the dry-etching process.

2. EXPERIMENT

The ultra-black absorber made from compressed-coal graphite plate ($10 \times 10 \times 1$ mm, Shuguang Carbon Industry Co., Ltd.) was fabricated by oxygen-plasma etching in an inductively coupled plasma reactive ion etching (ICP-RIE) system. The sample was placed on a silicon/silicon oxide wafer which provided the nanoparticle masks responsible for the formation of the structures. The reactive gas was pure oxygen (O_2) with a typical flow rate of 90 sccm. The ICP RF power and the RIE RF power were 100 W and 300 W respectively. The etching time was varied from 10 minutes to 60 minutes with a fixed chamber pressure of 30 mTorr.

The dimension and morphology of the structures were observed using top-view and tilt-view modes of the RAITH 2 scanning electron microscopy (SEM) operating at a 5 kV acceleration voltage. Optical reflectance measurements on the absorbers were carried out using three different optical measurement systems. The hemispherical (specular + diffuse) reflectance from 450 nm to 850 nm was measured using the Ocean Optics USB2000+UV-VIS spectrometer mounted with an integrating sphere ISP-REF. The reflectance was normalized to a standard white board. A Shimadzu UV-3101 spectrophotometer was used for characterizing the specular reflectance in the range from 850 nm to 1700 nm. A Bruker VERTEX 70 Fourier transform infrared (FTIR) spectrometer with an unpolarized light source was used to measure the specular reflectance with an Au mirror as the reference in the mid-infrared region. The minimum incident angle for specular reflectance measurement was 12 degrees in the FTIR system. X-ray photoelectron spectroscopy (XPS) was performed using the Thermo Fisher Escalab250Xi to characterize the elemental composition of the absorber surface.

3. RESULTS AND DISCUSSION

Etching a low quality graphite plate on top of a silicon substrate yields a surprisingly high quality ultrablack material through the formation of carbon nanoneedles beneath nanoscale silicon masks. Fig. 1 shows the tilt-view SEM images of the graphite-based absorbers with different etching times. The nanoneedle structures begin emerging from the surface after etching for 10 min (Fig. 1(d)). With increased etching time, the density and the height of the nanoneedles are increased. The graphite plates visual appearance becomes increasingly dark with increased etching times (Figs. 1(c)–(f) insets). We use tilt-view SEM to characterize the height and width of the nanoneedles for different etching times. The diameter of the nanoneedles is typically less than 100 nm for all the samples. For the height measurement, since silicon is continuously sputtered during the etching process, only the tallest nanoneedles indicate the height produced by the earliest masks in the etching process. The height of nanoneedles grows from 0 to around 5.7 μm at 60 minutes etching time. The graph in Fig. 1(b) shows that the height is generally linear in etching time.

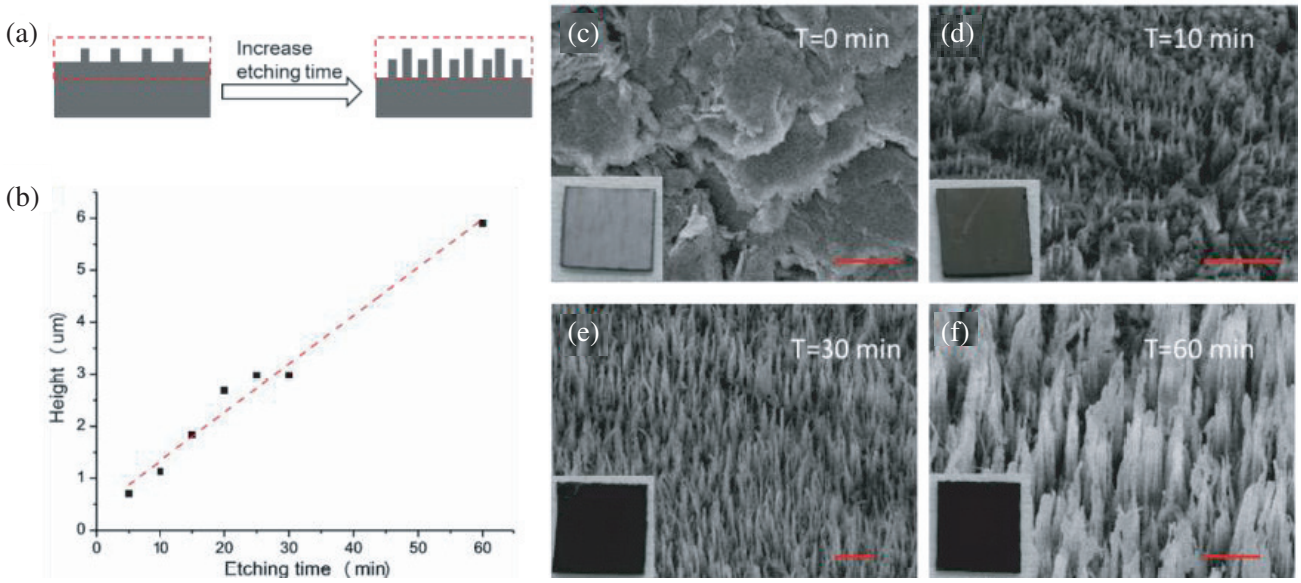

Figure 1. With additional etching time the density height, and polydispersity of the nanoneedles increase as schematically shown in (a). (b) The height of the tallest nanoneedles on a sample is linear in the etching time. The tilt-view SEM pictures for different etching times ((c) pristine, (d) 10 minutes, (e) 30 minutes and (f) 60 minutes) and the corresponding photographs (insets) show improved nanostructuring and visual blackness with increased etching time. Scale bar: 2 µm.

The reflectance spectra of the absorbers are characterized in the visible, near-IR, and mid-IR regions. In the visible regime (450–850 nm), the hemispherical (specular and diffuse) reflectance spectra was measured by a spectrometer with an integrating sphere attachment. As shown in Fig. 2(a), the total hemispherical reflectance of the absorber prepared with 60 minutes etching time is around 7%. As a comparison, the absorbers with etching time below 60 min show a higher reflectance above 1%. The specular reflectance of the absorbers across the near infrared (Fig. 2(b)) and mid infrared region (Fig. 2(c)) shows that the longer etched samples have improved absorption across all the wavelengths of interest. The reflectance of the absorber is well below 0.7% over the mid infrared range for the sample etched for 60 minutes. These results represent similar performance in the visible and near-IR when compared with pyrolytic carbon coated black silicon but better performance in the mid-IR [21]. Since the sum of reflectance (R), transmission (T), and absorption (α) equals 1 in thermal equilibrium, the absorption can be calculated as $\alpha = 1 - T - R$. The thickness of our samples is 1 mm, so we assume that zero transmission occurs. According to Fresnel's law, the reflectance on a boundary is determined by the impedance mismatch at the boundary:

$$R = (n - n_0)^2/(n + n_0)^2 \tag{1}$$

Consequently, the most critical design requirement for any ultrablack material is that there is a smooth transition between the impedance of the air and the impedance of the absorbing material. This is usually accomplished with tall narrow needle-like structures such as VANTA or relatively diffuse disordered materials. According to the effective medium theory [18], the effective refractive index of the surface can be calculated with a weighted average of the materials present:

$$n_{eff} = ff \cdot n_g + (1 - ff) \cdot n_0 \tag{2}$$

where ff is the filling factor of the nanoneedles, and n_g and n_0 are the complex refractive index of graphite and air. As the etching time increases, the height, density, and polydispersity of the nanoneedles will increase, and the filling factor will decrease which give a smaller effective refractive index of the surface (shown in Fig. 1(a)). As a result, it will produce a smoother impedance interface between the bulk graphite and air which results in a lower reflectance. Effective medium theory is only valid when the thickness considered is larger than the wavelength of light. When the wavelength becomes

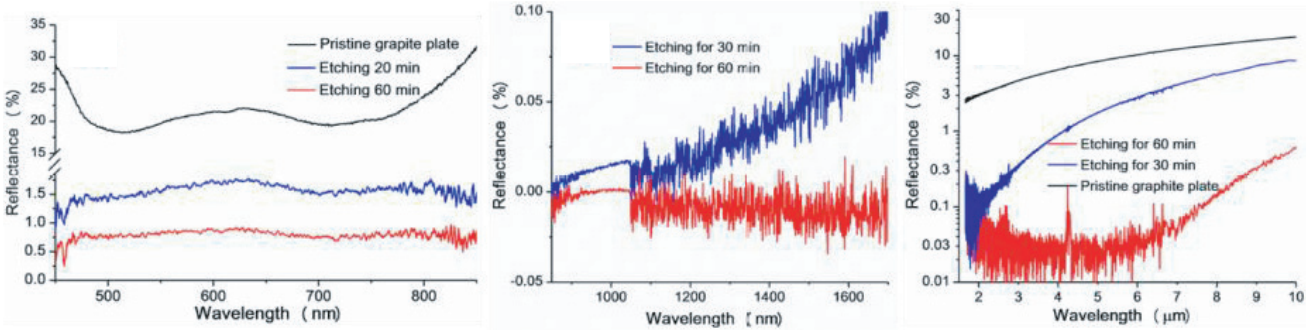

(a) (b) (c)

Figure 2. Spectral characterization (a) in the visible, (b) near infra-red and (c) mid infra-red shows the ultrablack quality of the prepared material. (a) The hemispherical reflectance of the device across the range from 450 nm to 850 nm shows that untreated graphite (black) reflects 20% of light, while the sample with 20 minutes etching (blue) reflects around 1.5% and the sample with 60 minutes etching (red) reflects around 0.7% of light. (b) The specular reflectance of the 60 minutes etched sample in the near-IR (red) is indistinguishable from 0, while the 20 minutes etched sample (blue) shows a characteristic growth in reflectance when the wavelength and needle size are similar reaching 0.1% at 1.7 microns. (c) Measured specular reflectance of the device at 12° across the range from 1.7 μm to 10 μm (c). The pristine graphite plate (black) shows a specular reflectance near 10% throughout the mid-IR, while the absorber with 30-minute etching (blue) has a specular reflectance that grows from 1% to 9% as the wavelength is tuned form 1.7 μm to 10 μm. The 60 minutes (red) etched sample shows relatively uniform specular reflectance of 0.03% until 6 μm and then grows to 0.7% by 10 μm.

comparable to the height of the tallest needles on a given sample, the reflection begins to grow since an effective medium calculation needs to include some of the solid substrate. The sample etched for 30 minutes shows this growth in reflectance around 1.2 μm (Fig. 2(b)), and the sample etched for 60 minutes shows this characteristic growth around 6 μm (Fig. 2(c)).

To understand the mechanism of nanoneedle formation, we use the XPS analysis to study the elemental composition. Fig. 3(a) shows survey scanning results for pristine compressed-coal graphite and the absorber after etching for 10, 20 and 30 minutes. The elemental composition determined from this XPS measurement is presented in Table 1. As the etching time increases, we see Silicon and Aluminum entering our material as a result of the self-masking process. Table 1 presents the atomic concentration of C, O, Si and Al. Little (∼ 1%) aluminum contamination appeared after 30 minutes of etching. Since the chamber and the clamping ring is made from aluminum, some aluminum may be sputtered during the dry-etching process. During the etching process the silicon and oxygen present on the surface of the graphite quickly saturate around 23% and 29% respectively. Since we run the oxygen plasma for a long time before fabricating our devices, silicon cannot come from the former recipe. Consequently, the only silicon source is the silicon/silicon oxide substrate wafer. During the etching process, the sputtering of silicon occurs on the silicon/silicon oxide wafer and some silicon particles are redeposited on the graphite plate surface (Fig. 3(b)). As a result, these silicon particles work as nano-masks during etching process. As the etching time increases, some silicon masks will be etched, and new silicon masks will deposit on the surface, which potentially accounts for the steady concentration of the silicon with etching time.

To confirm that the silicon was originating from the silicon wafer, a control experiment was conducted. Polyimide (PI) tape was used to cover the silicon wafer and prevent silicon sputtering during the oxygen etching. Then the PI-covered silicon wafer was used as the substrate in the ICP-RIE etching system. All other etching conditions were still the same with the absorbers during the process. As expected, after etching for 30 minutes, the etched graphite plate was still similar to the pristine one (Fig. 3(c)), which confirmed the self-mask effect was responsible for the nanoneedle formation. Since there was no mask on the graphite surface, no structure formed on it (Fig. 3(c)). This further supported that nanoneedle structures were the key factor for the high absorbance.

Table 1. Elemental composition of the samples determined by XPS.

Atomic %	C	O	Si	Al
Pristine graphite	93.04	6.96	-	-
Etching 10 min	46.24	29.64	24.12	-
Etching 20 min	48.84	28.75	22.41	-
Etching 30 min	47.22	28.96	22.71	1.11

The self-masked dry-etching method has been found in the electron cyclotron resonance (ECR) plasma system for varied materials by using carbon-based reactive gases [22]. During the process, reactive gases can react with the substrate and form carbon-based composites. These composites will act as masks among the etching process. Here we found that the self-mask effect can cause by the sputtering of the silicon substrate. Compared with these methods, our method only use oxygen as the reactive gas, which is safe, cheap, and environmentally friendly. Since the carbon is a naturally broadband absorber compared with silicon (which is transparent in the infrared regime), our graphite-based absorber shows a much wider absorption band than any pure silicon ultrablack material [23].

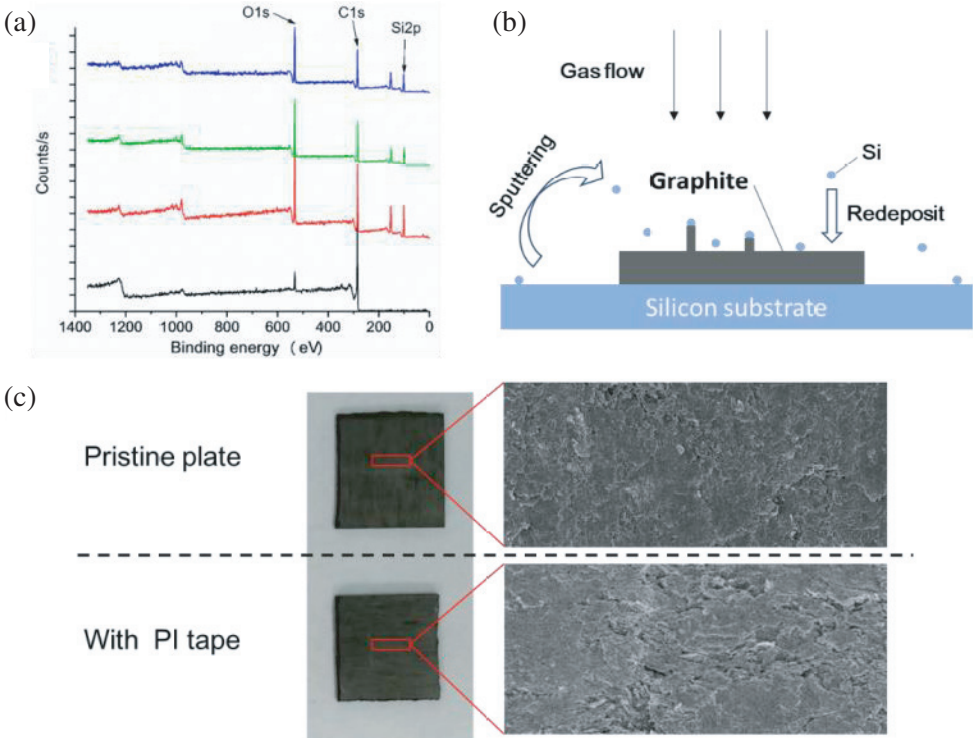

Figure 3. (a) The XPS survey scanning of the absorbers with etching time for 0 (black), 10 (red), 20 (green), 30 minutes (blue), which are summarized in Table 1. The gas flow during the etching process sputters silicon from the substrate onto the graphite which acts as the mask for the growth of the nanoneedles as schematically depicted in (b). (c) A control experiment where PI tape is used to cover the silicon substrate demonstrates that after 30 minutes of etching there is no noticeable effect on the graphite plate indicating that the silicon substrate is the source of the mask.

4. CONCLUSION

In summary, we fabricated a graphite-based ultra-black absorber by self-masked dry-etching method. The device shows reflectance below 0.7% from visible to infrared range (450 nm–10 μm), which is comparable to many more complicated ultrablack material systems and a broader band than pure silicon ultrablack materials can achieve. These structures are the consequence of silicon sputtering and redisposition during the etching process. This one-step technique makes it possible to fabricate a scalable ultrablack material. Since the graphite is an abundant and cheap material in nature, this device is very promising for mass production to meet applications such as thermal management and thermal imaging.

ACKNOWLEDGMENT

This work was supported by the National Natural Science Foundation of China (Nos. 61550110246 and 11621101) and the Science and Technology Department of Zhejiang Province (2010R50007).

REFERENCES

1. Kuhn, T. S., *Black-body Theory and the Quantum Discontinuity*, 1894–1912, University of Chicago Press, Chicago, 1987.
2. Hagopian, J. G., S. A. Getty, M. Quijada, J. Tveekrem, R. Shiri, P. Roman, J. Butler, G. Georgiev, J. Livas, and C. Hunt, "Multiwalled carbon nanotubes for stray light suppression in space flight instruments," *Proc. SPIE*, 2010.
3. Theocharous, E., C. J. Chunnilall, R. Mole, D. Gibbs, N. Fox, N. Shang, G. Howlett, B. Jensen, R. Taylor, and J. R. Reveles, "The partial space qualification of a vertically aligned carbon nanotube coating on aluminium substrates for EO applications," *Opt. Express*, Vol. 22, No. 6, 7290–7307, 2014.
4. Kodama, S., M. Horiuchi, K. Kuroda, and T. Kunii, "Ultra-black nickel-phosphorus alloy optical absorber," *6th IEEE Instrumentation and Measurement Technology Conference, 1989, IMTC-89*, 1989.
5. Brown, R. J., P. J. Brewer, and M. J. Milton, "The physical and chemical properties of electroless nickel-phosphorus alloys and low reflectance nickel-phosphorus black surfaces," *J. Mater. Chem.*, Vol. 12, No. 9, 2749–2754, 2002.
6. Yang, Z.-P., L. Ci, J. A. Bur, S.-Y. Lin, and P. M. Ajayan, "Experimental observation of an extremely dark material made by a low-density nanotube array," *Nano Lett.*, Vol. 8, No. 2, 446–451, 2008.
7. Mizuno, K., J. Ishii, H. Kishida, Y. Hayamizu, S. Yasuda, D. N. Futaba, M. Yumura, and K. Hata, "A black body absorber from vertically aligned single-walled carbon nanotubes," *Proc. Natl. Acad. Sci.*, Vol. 106, No. 15, 6044–6047, 2009.
8. Zhou, L., Y. Tan, D. Ji, B. Zhu, P. Zhang, J. Xu, Q. Gan, Z. Yu, and J. Zhu, "Self-assembly of highly efficient, broadband plasmonic absorbers for solar steam generation," *Science Adv.*, Vol. 2, No. 4, e1501227, 2016.
9. Lenert, A., D. M. Bierman, Y. Nam, W. R. Chan, I. Celanović, M. Soljačić, and E. N. Wang, "A nanophotonic solar thermophotovoltaic device," *Nat. Nanotechnol.*, Vol. 9, No. 2, 126–130, 2014.
10. Lehman, J., A. Sanders, L. Hanssen, B. Wilthan, J. Zeng, and C. Jensen, "Very black infrared detector from vertically aligned carbon nanotubes and electric-field poling of lithium antalate," *Nano Lett.*, Vol. 10, No. 9, 3261–3266, 2010.
11. Theocharous, E., R. Deshpande, A. Dillon, and J. Lehman, "Evaluation of a pyroelectric detector with a carbon multiwalled nanotube black coating in the infrared," *Appl. Opt.*, Vol. 45, No. 6, 1093–1097, 2006.
12. Mellouki, I., N. Bennaji, and N. Yacoubi, "IR characterization of graphite black-coating for cryogenic detectors," *Infrared Phys. Technol.*, Vol. 50, No. 1, 58–62, 2007.

13. Granqvist, C., "Radiative heating and cooling with spectrally selective surfaces," *Appl. Opt.*, Vol. 20, No. 15, 2606–2615, 1981.
14. Her, T.-H., R. J. Finlay, C. Wu, S. Deliwala, and E. Mazur, "Microstructuring of silicon with femtosecond laser pulses," *Appl. Phys. Lett.*, Vol. 73, No. 12, 1673–1675, 1998.
15. Peng, K.-Q., Y.-J. Yan, S.-P. Gao, and J. Zhu, "Synthesis of large-area silicon nanowire arrays via self-assembling nanoelectrochemistry," *Adv. Mater.*, Vol. 14, No. 16, 1164, 2002.
16. Jansen, H., M. de Boer, R. Legtenberg, and M. Elwenspoek, "The black silicon method: A universal method for determining the parameter setting of a fluorine-based reactive ion etcher in deep silicon trench etching with profile control," *JMiMi*, Vol. 5, No. 2, 115, 1995.
17. Sun, Y., J. Evans, F. Ding, S. Wang, L. Mo, and S. He, "Patterning of graphite nanocones for broadband solar spectrum absorption," *AIP Adv.*, Vol. 5, No. 6, 067139, 2015.
18. Sun, Y., J. Evans, F. Ding, N. Liu, W. Liu, Y. Zhang, and S. He, "Bendable, ultra-black absorber based on a graphite nanocone nanowire composite structure," *Opt. Express*, Vol. 23, No. 15, 20115–20123, 2015.
19. Letellier, M., J. Macutkevic, P. Kuzhir, J. Banys, V. Fierro, and A. Celzard, "Electromagnetic properties of model vitreous carbon foams," *Carbon*, Vol. 122, 217–227, 2017.
20. Kuzhir, P. P., A. G. Paddubskaya, N. I. Volynets, K. G. Batrakov, T. Kaplas, P. Lamberti, R. Kotsilkova, and P. Lambin, "Main principles of passive devices based on graphene and carbon films in microwave-THz frequency range," *J. Nanophotonics*, Vol. 11, No. 3, 032504–032504, 2017.
21. Shah, A., P. Stenberg, L. Karvonen, R. Ali, S. Honkanen, H. Lipsanen, N. Peyghambarian, M. Kuittinen, Y. Svirko, and T. Kaplas, "Pyrolytic carbon coated black silicon," *Sci. Rep.*, Vol. 6, No. 1, 25922, 2016.
22. Hsu, C.-H., H.-C. Lo, C.-F. Chen, C. T. Wu, J.-S. Hwang, D. Das, J. Tsai, L.-C. Chen, and K.-H. Chen, "Generally applicable self-masked dry etching technique for nanotip array fabrication," *Nano Lett.*, Vol. 4, No. 3, 471–475, 2004.
23. Huang, Y.-F., S. Chattopadhyay, Y.-J. Jen, C.-Y. Peng, T.-A. Liu, Y.-K. Hsu, C.-L. Pan, H.-C. Lo, C.-H. Hsu, and Y.-H. Chang, "Improved broadband and quasi-omnidirectional anti-reflection properties with biomimetic silicon nanostructures," *Nat. Nanotechnol.*, Vol. 2, No. 12, 770–774, 2007.